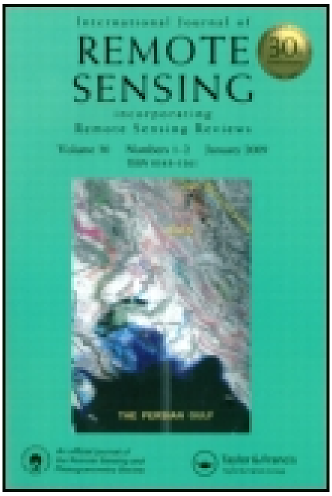

International Journal of Remote Sensing
Publication details, including instructions for authors and subscription information:
http://www.tandfonline.com/loi/tres20

Comparison of different techniques in atmospheric temperature-humidity sensing from space

Alexander Polyakov[a], Yurii M. Timofeyev[a] & Yana Virolainen[a]
[a] Department of Atmospheric Physics, Saint Petersburg State University, Sankt-Petersburg-Petrodvorets, Russian Federation
Published online: 28 Aug 2014.

To cite this article: Alexander Polyakov, Yurii M. Timofeyev & Yana Virolainen (2014) Comparison of different techniques in atmospheric temperature-humidity sensing from space, International Journal of Remote Sensing, 35:15, 5899-5912

To link to this article: http://dx.doi.org/10.1080/01431161.2014.945004

International Journal of Remote Sensing, 2014
Vol. 35, No. 15, 5899–5912, http://dx.doi.org/10.1080/01431161.2014.945004

Comparison of different techniques in atmospheric temperature-humidity sensing from space

Alexander Polyakov*, Yurii M. Timofeyev, and Yana Virolainen

Department of Atmospheric Physics, Saint Petersburg State University, Sankt-Petersburg-Petrodvorets, Russian Federation

(*Received 19 July 2013; accepted 9 March 2014*)

Numerical closed-loop experiments on retrieving atmospheric temperature and humidity profiles by high-resolution measurements of the outgoing thermal infrared (IR) radiation using a Russian Fourier spectrometer (IRFS-2) were performed. Three techniques were used: multiple linear regression (MLR), the iterative physical-mathematical approach (IPMA), and artificial neural networks (ANNs). The MLR technique gives significant root mean square (RMS) errors in the retrieval of the temperature profile, especially in the troposphere region; these errors may be as great as 2–3 K. The ANN and IPMA techniques are considerably more accurate, giving approximately equal RMS errors of 1.0–1.5 K at altitudes of 2–30 km. For all interpretation techniques, a growth of errors of retrieval of temperature in the lower troposphere is observed and is especially substantial (up to 3 K for the near-surface temperature) in thermal sensing over land. The systematic errors of temperature retrieval for the ANN technique are practically zero, and for the other two techniques, they do not exceed 0.4 K. The differences in thermal sensing of the atmosphere over water and land manifest themselves in the appearance of an additional five determined coefficients of expansion of the spectral dependence of the IR emissivity of land in principal components. This leads to increased errors on thermal sensing in the lower troposphere, up to ~0.5 K for all interpretation techniques. The information content of the IRFS-2 device measurements with regard to the atmospheric humidity profile is relatively small because of the values of the errors of measurements of the outgoing radiation in the shortwave range, and in particular, in the water vapour absorption band 6.3 μm. The ANN technique makes it possible to determine relative humidity in the troposphere with RMS errors of 10–15%. In the case of observations over water, the mean errors of the ANN technique are practically equal to zero, and for the MLR and IPMA techniques, they are of an approximately equal order of magnitude, namely 2–4% of relative humidity. The IPMA and MLR techniques give RMS humidity errors of 15–20% and up to 40%, respectively.

1. Introduction

Although the development of techniques of atmospheric temperature and humidity sounding (THS) from space has a history of over 50 years (King 1956; Kaplan 1959; Kondratyev and Timofeev 1970), improvement of this important remote-sensing method is actively continuing. In recent years, new efforts have been made to satisfy the high requirements for the accuracy and vertical resolution of retrieval of vertical profiles of atmospheric temperature and humidity. These efforts are, in particular, connected with the creation and exploitation of multi-channel devices of relatively high spectral resolution, for measuring, with high precision, the outgoing thermal radiation in a wide infrared (IR) spectral range. (The atmospheric infrared sounder (AIRS), the infrared atmospheric

*Corresponding author. Email: polyakov@troll.phys.spbu.ru

sounding interferometer (IASI), cross-track infrared sounder (CrIS) devices; Aumann et al. 2003; Pougatchev et al. 2009; Smith et al. 2009.) The purpose of this approach is to use the information contained in the outgoing thermal radiation to the maximum possible extent, as well as to increase spatial (vertical) resolution by narrowing the weight functions (Smith et al. 2009). Undoubtedly, this approach has proved to be substantially successful, as it made it possible to improve the quality of atmospheric temperature-humidity sounding and also to obtain important additional information, such as on the gas composition of the atmosphere (see, for example, Clerbaux et al. 2009; Coheur et al. 2009).

When using thousands of spectral channels, the problem of the speed of performance of the programs of real-time satellite measurement processing arises. This is first of all connected with the demands of numerical weather forecasting. One way to solve the performance speed problem is by using regression approaches, particularly multiple linear regression (MLR) or artificial neural networks (ANNs). The latter approach is usually used to solve nonlinear inverse problems, and its efficiency is demonstrated by Frate and Schiavon (1998), Krasnopolsky, Gemmill, and Breaker (2000), Aires et al. (2001, 2002a, 2002b), Gribanov and Zakharov (2003), Blackwell, Frederick, and Chen (2005), Karbou et al. (2005), Blackwell, Pieper, and Jairam (2008) and Wang et al. (2013).

In Russia, an infrared Fourier spectrometer for the measurement of the outgoing thermal radiation in the spectral range of 667–2000 cm^{-1} with a spectral resolution of 0.4–0.7 cm^{-1} was created (Zavelevich, Golovin, and Desyatov 2009). The advanced IR sounder IRFS-2 (InfraRed Fourier Spectrometer-2), designed and manufactured by the Keldysh Centre (Roskosmos), is planned to be launched aboard the 'Meteor-3M' N 2 satellite. The IRFS has a somewhat reduced spectral measurement range compared with other satellite devices, but it includes the most important absorption bands of CO_2, O_3, H_2O, and other gases. We get spectra with a fixed spectral resolution of 0.7 cm^{-1} in the spectral region 667–1200 and 1.4 cm^{-1} in other spectral regions with a Gaussian slit function.

To reduce the time required to interpret large amounts of satellite measurements, various ways of increasing the efficiency of data processing are used.

- Development of high-speed techniques and algorithms for calculating the outgoing radiation, i.e. for solving the direct problem (for example, Matricardi and Saunders 1999; Matricardi 2004).
- Compression of spectral radiation information, using approximations by expansion in principal components (PCs) (Huang and Antonelli 2001; Aires et al. 2002; Uspenskiy, Romanov, and Trotsenko 2003).
- Use, at the first stage of measurements analysis, of multiple linear regression (MLR);
- Reduction of the number of spectral measurement channels used by selecting a limited number of optimal channels or creating combined 'super-channels' (see, for example, Liu et al. 2009).
- Use of the technique of principal components (PCs) in the space of the sought profiles, i.e. transition, in solving inverse problems, to approximations of the profiles being sought, by empirical orthogonal functions (EOF) expansion.
- Use of a double regression technique applied for the interpretation of CrIS measurements (see, for example, Smith et al. 2012).

For the Russian device, specialized software was earlier developed using the MLR techniques and the iteration physics-mathematical approach (IPMA) based on the optimal estimation method (Polyakov, Timofeyev, and Uspenskiy 2009, 2010; Virolainen et al. 2010). At the first stage of measurement processing, the MLR fast technique was used, and after the analysis of the residual between the measured and calculated spectral thermal radiation, the IPMA was applied.

Numerical simulation has shown that the use of the MLR technique at the first stage of analysing the satellite data often requires the application of the second stage of the solution process, i.e. the nonlinear solution of the problem, especially in retrieving the atmospheric humidity profile. This leads to a significant increase of the time required to process the satellite measurements. Therefore, it is expedient to consider the possibilities of using the ANN technique, instead of MLR, at the first stage of satellite measurements processing.

The second section of the article describes the specific features of the elaboration of the operator of the inverse problem solution, an operator which is based on application of the ANN technique. These specific features include the used ensemble of the atmosphere-surface system states and selection of the number of principal components. The following section briefly describes the two other methods of inverse problem solving, MLR and IPMA. The fourth section of the article is devoted to analysis of numerical experiments on temperature-humidity sensing of the atmosphere by the use of the three techniques of interpretation. In the final section, the main results of the investigation and the conclusions obtained are given.

2. Elaboration of artificial neural networks

The ANN technique for atmospheric temperature-humidity satellite measurements was tested in closed-loop numerical experiments. For each physical state of the atmosphere-surface system from a large set of states, calculations of the outgoing radiation spectra were made, based on the algorithm of the direct problem solution, taking into account the spectral slit function of the device.

Furthermore, to obtain the 'measured radiation spectra', the influence of the measurement error was modelled. The 'measured radiation spectra' obtained were used in solving the inverse problem by the ANN and other techniques. The solution of the inverse problem and the initial implementation of the state of the atmosphere-surface system were compared to estimate the quality of the solution of the inverse problem – calculation of the mean and root mean square (RMS) errors of the temperature and humidity profile retrieval. Following the vast majority of publications on applying ANNs in the inverse problems of atmospheric optics, in solving the inverse problem under consideration, we chose a three-layer perceptron (or, in another terminology, a network with one hidden layer). Figure 1 shows a graphical representation of the chosen network.

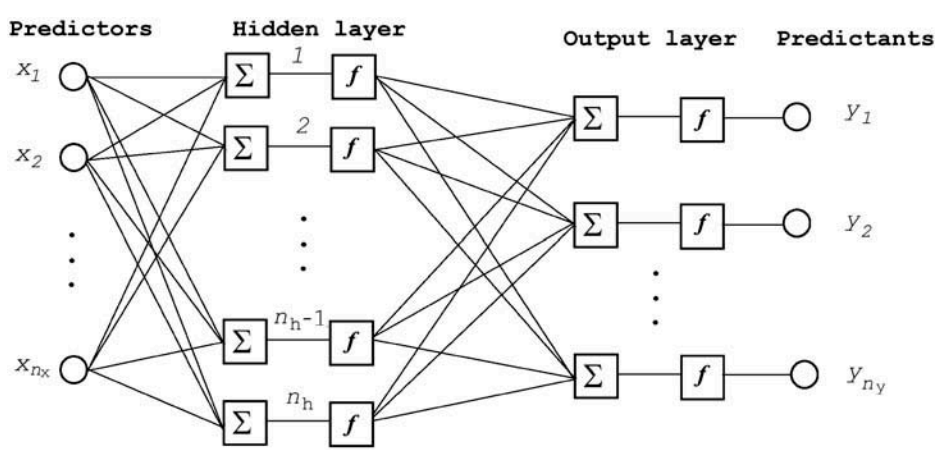

Figure 1. Scheme of three-layer perceptron.

There we used an original method of ANN training, which is described in detail by Polyakov (2014). Let us consider the different components which are necessary to carry out the numerical experiments.

2.1. Database of the atmosphere-surface states

An essential role in constructing, debugging, and testing the systems for interpreting remote measurements is played by the selection of a set of model states of the atmosphere, also called a statistical model or database of the state of the atmosphere. The properties of this set are especially important in the case of using it to construct the regression solving operators of the inverse problem (the MLR and ANN techniques). The task of statistical modelling of the parameters of the state of the atmosphere and the surface characteristics was formulated as follows: to form the sets of vertical profiles of temperature and humidity of the atmosphere and the surface characteristics (temperature and emissivity) in the altitude interval of 0–80 km, sets which should adequately describe the observed global variations and correlations of these parameters. As the basis for constructing the statistical model of the atmosphere, we chose the Thermodynamic Initial Guess Retrieval (TIGR) database (Chedin et al. 1985), widely known and used earlier by a number of authors. In spacing the altitude in the troposphere region, the minimal spacing was used (0.5 km), based on the current WMO requirements on the vertical resolution of temperature sounding in the troposphere (1 km). For the stratosphere and mesosphere regions, the spacing gradually increases, reaching 2.5 km at altitudes of 70–80 km. The database was randomly divided into two parts: training and a test sample, in the proportion of 85:15.

The profiles of the TIGR database, which contains vertical profiles of temperature, as well as water vapour and ozone content, up to an altitude of about 72 km, relate to different latitude zones and types of state of the atmosphere. In the altitude range of 72–80 km, the profiles of temperature, water vapour, and ozone content were built up by using the profiles from the AFGL86 model (Anderson et al. 1986).

The set of the parameters of the database formed additionally included the following: for the underlying land surface, the land temperature T_s and the spectral dependence of the IR emissivity $\varepsilon(v)$, where ε is emissivity and v is wavenumber, T_s differing from the temperature of the atmosphere near the surface; for the water surface, the water temperature and the spectral dependence $\varepsilon(\nu)$, which was set according to Nalli, Smith, and Huang (2001).

For simulation of the inverse problem of retrieval of the land surface temperature and its emissivity $\varepsilon(v)$, we use the technique suggested in Timofeyev and Martynov (1996) and the data kindly provided to us by Dr Jack Salisbury (Dept. of Earth and Planetary Sciences, Johns Hopkins University), which are measurements of the spectral dependence of the emissivity of various types of land surface in the range 7.5–14 μm. Having constructed the covariance matrix of the experimental ensemble $\varepsilon(v)$, we calculated its eigenvectors and eigenvalues. Using the expansion of the emissivity spectral curve in the eigenvectors of the covariance matrix, we constructed the optimal parameterization of $\varepsilon(v)$ and calculated the error of this approximation, based on the example of the same ensemble of experimental data. In our algorithm we used five principal components of the spectral curve of the surface emissivity, which makes it possible to approximate the emissivity with an error less than 1%.

2.2. Selection of the number of principal components

Selection of the number of principal components in the parameterization of vertical profiles of temperature $T(z)$ and humidity $R_H(z)$ was carried out on the basis of comparing

Table 1. RMS errors of expansion of profiles of temperature $T(z)$ and relative humidity $R_{\mathrm{H}}(z)$, %, in truncated EOF bases with respect to the basis dimension (the number of PCs).

Number of PCs	1	5	10	11	12	13	14	15	16	17	18	19
$T(z)$ (K)	8.81	2.21	0.87	0.74	0.64	0.56	0.49	0.43	0.38	0.34	0.29	0.26
$R_H(z)$ (%)	19.3	7.9	3.9	3.5	3.2	2.8	2.5	2.2	2.0	1.8	1.6	1.5

the errors of parameterizations with potential errors of the inverse problem solution. Parameterization errors of vertical profiles of temperature and relative humidity for several different numbers of PCs are given in Table 1.

Based on the analysis of RMS errors presented in Table 1, a decision was taken to use 17 and 13 PCs for the parameterization of vertical profiles of temperature and humidity, respectively. In this case, the growth of the total error of remote sensing because of the errors of parameterization of temperature and humidity profiles is less than 10%.

In selecting the number of PCs in the parameterization of spectra of the outgoing radiation measured by the IRFS-2 device (the total number of measurements over a spectra is equal 2701), the results of Virolainen et al. (2010) were used, in which it is shown that for temperature-humidity sensing at the errors of IRFS-2 measurements, 40 PCs are sufficient for the parameterization of the outgoing radiation spectra in the spectral measurement range.

3. Other techniques of solving the inverse problem

The elaborated program of ANN interpretation of satellite measurements of the IRFS-2 device was compared with other techniques of solving this inverse problem. Let us introduce the following designations: $\boldsymbol{\varphi}$ is the vector of the sought variables, in which we combine all values determined in solving the inverse problem, namely, profiles of temperature and water vapour mixing ratios (or relative humidity), surface temperature, and coefficients of expansion on the basis of the function of the spectral dependence of IR emissivity of the land surface; $\boldsymbol{f}$ is the vector of measurements, that is, radiation values measured by the device.

3.1. Multiple linear regression

In using the MLR technique, the nonlinear problem is linearized on the average vector of the parameters, which describe the atmosphere-surface system. We will designate the cross-covariance matrix of such vectors as $K_{\varphi f}$, and the covariance matrix of measurements, which also includes measurement errors, as K_f. Then the expression for the matrix of the solving operator R can be written in the form

$$R = K_{\varphi f} K_f^{-1} \tag{1}$$

and the estimation of the solution $\tilde{\boldsymbol{\varphi}}$ is described by the expression

$$\tilde{\boldsymbol{\varphi}} = \bar{\boldsymbol{\varphi}} + \mathbf{R}(\boldsymbol{f} - \bar{\boldsymbol{f}}), \tag{2}$$

where $\bar{\boldsymbol{f}}$ and $\bar{\boldsymbol{\varphi}}$ are average values of the vectors of the measured and sought values. It should be noted that to apply this method in practice, with constructing the solving operator, it is necessary, first of all, to have a sample of pairs $\{\boldsymbol{\varphi},\boldsymbol{f}\}$ of a sufficiently large volume. Let us make a point of the regularizing role of the measurement error. It is important to note that for calculating matrices $K_{\varphi f}$ and K_f, random measurement noise was added to the spectra.

This value functions as regularization in inversion of the matrix K_f, which is essentially important, since in using calculated values without the addition of noise, the matrix turns out to be singular.

3.2. *Iteration technique based on the physical-mathematical approach*

The IPMA technique solves the nonlinear inverse problem on the basis of the integral form of the radiation transfer equation. After solving the inverse problem by the MLR or ANN technique, based on the solution obtained, the radiation spectrum was calculated and was compared with the measured one. If the RMS difference between the spectra exceeded a chosen value, then the solution was improved by the IPMA technique. The essence of the algorithm is linearization, at each step of the algorithm, of the solution of the direct operator $\mathbf{B}$ (the problem $\boldsymbol{f}+\boldsymbol{\varepsilon}=\mathbf{B}(\boldsymbol{\varphi})$) in the neighbourhood of the preceding approximation of the solution and application of the statistical regularization method

$$\boldsymbol{x}_{k+1}=\bar{\boldsymbol{x}}+\left(\mathbf{A}_k{}'\Sigma^{-1}\mathbf{A}_k+\mathbf{D}^{-1}+\mathbf{L}^{-1}\right)^{-1}$$

$$\times\left(\mathbf{A}_k{}'\Sigma^{-1}(\tilde{\boldsymbol{y}}-\mathbf{B}(\boldsymbol{x}_k)+\mathbf{A}_k(\boldsymbol{x}_k-\bar{\boldsymbol{x}}))+\mathbf{L}(\boldsymbol{x}_k-\bar{\boldsymbol{x}})\right), \tag{3}$$

where $\mathbf{A}_k$ is the matrix of the derivatives of the operator $\mathbf{B}$ in the point $\boldsymbol{x}_k$, $\mathbf{D}$ is a priory matrix, $\tilde{\boldsymbol{y}}$ is the measured spectra, and Σ is the spectra measurement error matrix. Since it is not known in advance how close the problem operator $\mathbf{B}$ is to the linear one, it may be necessary to limit the change of the solution at each step of the iteration process (Polyakov 1996). For this, we introduce one more item in the iterative solution algorithm, the last item in Equation (3). Here $\mathbf{L}$ is any positive definite matrix that sets the correspondent norm. It should be noted that, on the one hand, the introduced item limits the difference $\boldsymbol{x}_{k+1}-\boldsymbol{x}_k$, i.e. change of the solution at one step of the iteration process, and, on the other hand, at solution convergence this difference tends to zero. Thus, the iteration process corresponding to Equation (3) leads to the solution of the inverse problem at selection of matrix $\mathbf{L}$ that will secure convergence of the process.

The convergence criterion is the fulfilment of at least one of the following conditions:

(1) convergence of the solution in itself; more exactly, satisfaction of the inequality $\left\|\tilde{\vec{x}}_{k+1}-\tilde{\vec{x}}_k\right\|_{\tilde{\mathbf{D}}^{-1}}<0.0001$, where $\tilde{\mathbf{D}}$ is an error matrix,

(2) the value of the norm residual $\sqrt{1/m\left\|\mathbf{B}(\tilde{\vec{x}})-\tilde{\vec{y}}\right\|^2_{\Sigma^{-1}}}$, where m is number of spectral channels, is less than 1, or

(3) the number of iterations has reached the limit set (5 here).

As a result, in the vast majority of cases, the number of iterations which are necessary to achieve convergence of the solution is 2–3; only in 5–10% of the cases were up to 5 iterations needed.

Unlike the ANN and MLR approaches, in the IPMA we use only some of the spectral channels of the IRFS-2. Eighty-one spectral channels were used to retrieve the temperature profile, 10 channels were used to retrieve the humidity profile and ozone, and 20 channels were used for surface temperature and emissivity. The channel selection was based on the information content of the measurement calculation and some spectra analysis.

4. Analysis of the results of numerical experiments

Numerical experiments on simulating the problem of temperature-humidity sensing by means of the IRFS-2 device were carried out for a test sample of temperature and humidity profiles of the test part of the database. As the characteristics of sensing accuracy, the following values were used:

– mean (systematic) disagreement $M = \frac{1}{N} \sum_{i=1,N} (x_i - y_i)$,

– RMS disagreement, $S = \sqrt{\frac{1}{N} \sum_{i=1,N} (x_i - y_i)^2}$,

where x_i and y_i are the accurate and retrieved values of the temperature and humidity of the atmosphere.

Figure 2 shows the mean and RMS disagreements of the entire ensemble of comparisons of temperature profiles of the numerical experiments. The mean errors for the MLR techniques are 0.1–0.4 K, while for the IPMA, they are considerably lower, 0.1–0.2 K. For the ANN, the mean (systematic) errors are practically equal to zero. The RMS

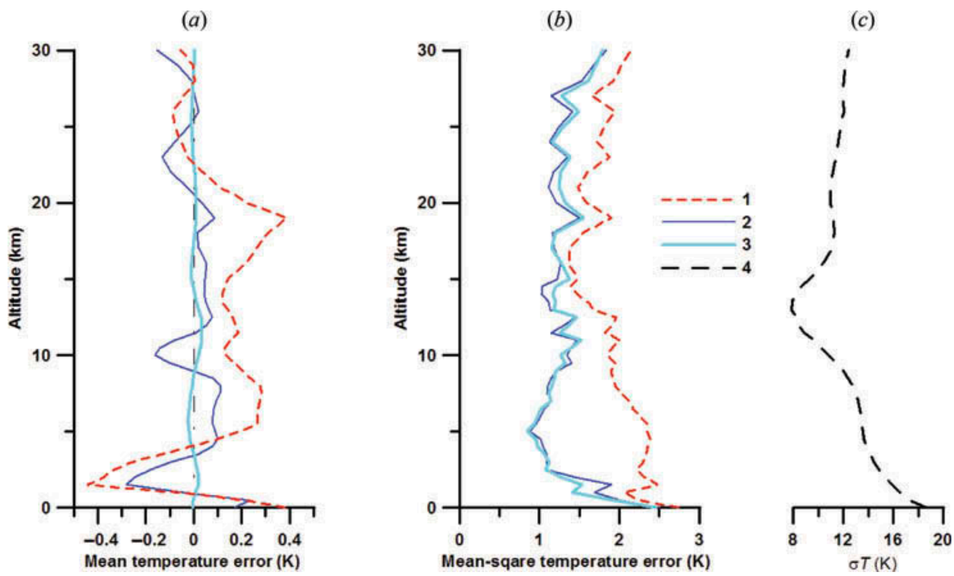

Figure 2. Mean (a) and mean-square (b) errors of estimation of temperature profile over water. Curve 1, MLR technique; curve 2, IPMA technique; curve 3, ANN technique; curve 4, *a priori* variability of temperature σT (c).

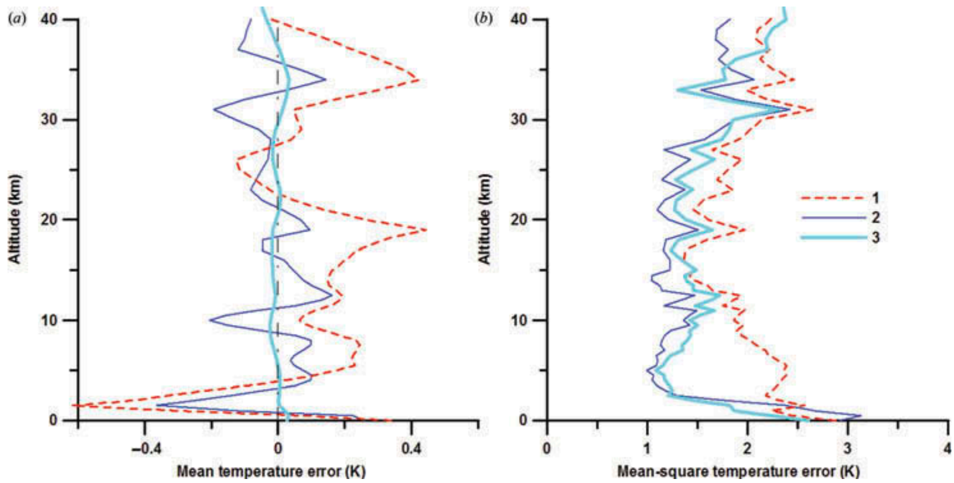

Figure 3. Mean (*a*) and mean-square (*b*) errors of estimation of the temperature profile over land. Curve 1, MLR technique; curve 2, IPMA technique; curve 3, ANN technique.

disagreements are maximal when using the MLR techniques at altitudes of 0–10 km, where they are 2 K or more. The two other techniques (IPMA and ANN) give approximately equal results; the RMS disagreements at altitudes of 2–30 km are close to 1–1.5 K. Note that the natural (*a priori*) variability of temperature for the temperature profiles under consideration is 8–18 K at different altitudes. All techniques give rather low accuracy of temperature retrieval in the lower troposphere. These errors near the water surface reach approximately 2.5 K.

Figure 3 presents the same characteristics as in Figure 2, but for observations over land. In this case, the number of parameters determined increases due to the characteristics of the emissivity of the surface in the form of five unknown coefficients of the expansion of emissivity of land $\varepsilon(\nu)$ in PCs. For the case of land, the systematic errors for the MLR and IPMA techniques noticeably increase near the surface. The ANN technique again has practically no systematic errors. The RMS disagreements also increase near the Earth's surface, reaching ~3 K for all three interpretation techniques. The increase, by contrast with the case of the water surface, is observed at all other altitudes as well; however, it has relatively small values: 0.1–0.3 K. Similarly to the case of the water surface, the MLR technique gives noticeably higher errors in the troposphere, as compared to the other two; the differences are 0.5–1.0 K. In the stratosphere, the differences between the results given by the different techniques are not large, at 0.2–0.4 K. At most altitudes, the IPMA techniques have some advantage, although the ANN techniques produce results differing by about 0.2 K.

Let us consider the error distribution in temperature retrieval on several typical levels in the atmosphere. For example, the RMS errors for the 5 km altitude for the IPMA and ANN techniques are practically equal, 0.90 K and 0.85 K, whereas for the MLR technique, it is 2.3 K. The figures presented demonstrate the variability of the errors of temperature retrieval, for both different techniques and different realizations of the temperature state of the atmosphere.

Let us consider the results of the numerical experiments on retrieval of the humidity profile in the troposphere. First of all, note the differences in retrieval of the characteristics of atmospheric humidity in different interpretation techniques. In the MLR and ANN

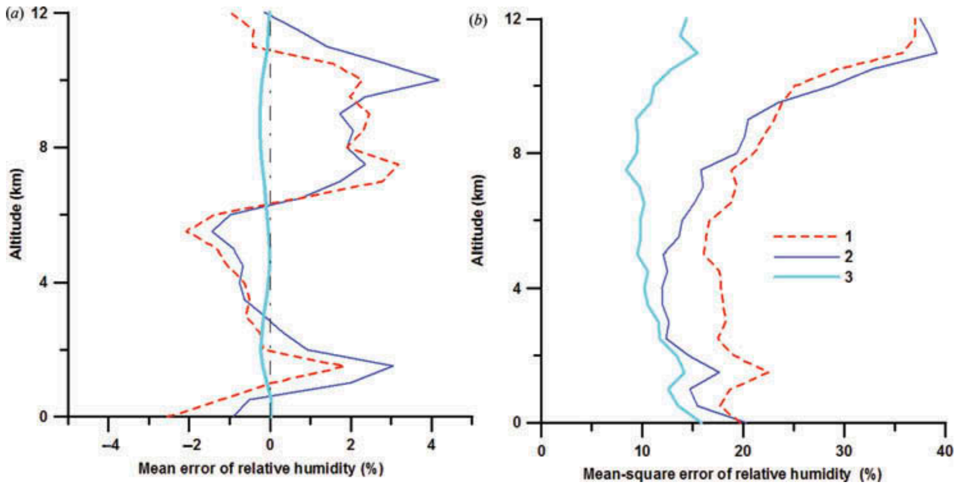

Figure 4. Mean (*a*) and RMS (*b*) errors of estimation of relative humidity profile in the troposphere over water. Curve 1, MLR technique; curve 2, IPMA technique; curve 3, ANN technique.

techniques, the inverse operator is constructed directly with respect to the relative humidity of the atmosphere. In the consequent use of the MLR and IPMA techniques, for MLR at the first stage, the profiles of the water vapour mixing ratio are found, and then, with the addition of atmospheric temperature data, relative humidity is determined.

In the case of observations over water (Figure 4), the mean errors for the MLR and IPMA techniques are approximately the same order of magnitude, at 2–4% of relative humidity. For the ANN technique, these errors are practically zero. The RMS errors are maximal for the MLR technique: 20–40% at altitudes of 0–12 km. It is obvious that this is caused by the significant nonlinearity of the problem for these conditions. The iterative approach is much more accurate at altitudes up to 8 km, and the errors for these altitudes are close to 15%. These two techniques are characterized by significant growth of the errors of relative humidity retrieval in the upper troposphere at altitudes of 10–12 km. At these altitudes, the errors reach 40%. Considerably smaller errors of retrieval of relative humidity are observed in using the ANN technique on the whole range of altitudes of 0–12 km. The RMS errors are 10–15%.

It should be noted that the relatively high errors of retrieval of relative humidity by means of the IRFS-2 measurements are caused by growth of the relative error of measurements of the outgoing thermal radiation in the shortwave measurement range, particularly in the water vapour band at 6.3 μm. These errors in the 6.3 μm band are 2–3 times higher than, for example, in measurements of the IASI and CrIS devices.

In outline, the specific features of the behaviour of the errors of retrieval of relative humidity over land are similar to the Figure 4 observations over water. Thus, mean errors for the MLR and IPMA techniques are within the range 0–4% of relative humidity. The ANN technique does not have systematic errors. The RMS errors are minimal for the ANN technique, at 10–15%. The second in accuracy is the IPMA technique (15–20% at altitudes of 0–8 km) and then the MLR, with 20–25% at these altitudes. In the upper troposphere, the errors reach 30–38% for these two techniques.

The distributions of the errors of retrieval of relative humidity of the atmosphere over water in the layer centred at 7.5 km for different techniques of interpretation are presented in Figures 5 and 6. Figure 5 demonstrates a comparison of the errors of the two

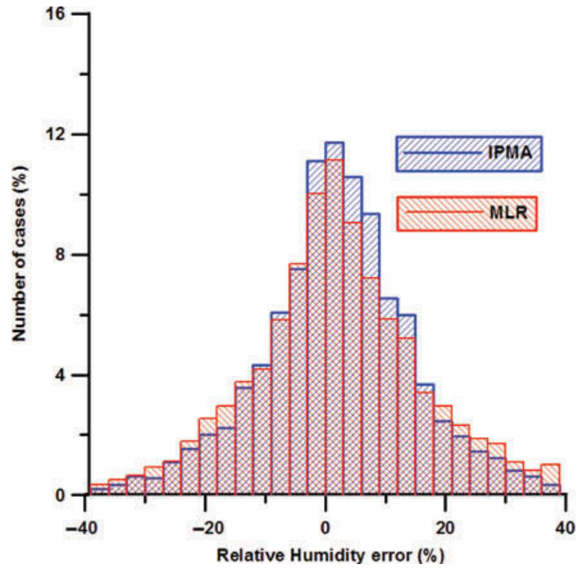

Figure 5. Distribution of errors of relative humidity retrieval at the 7.5 km altitude over water by means of two interpretation techniques, IPMA and MLR.

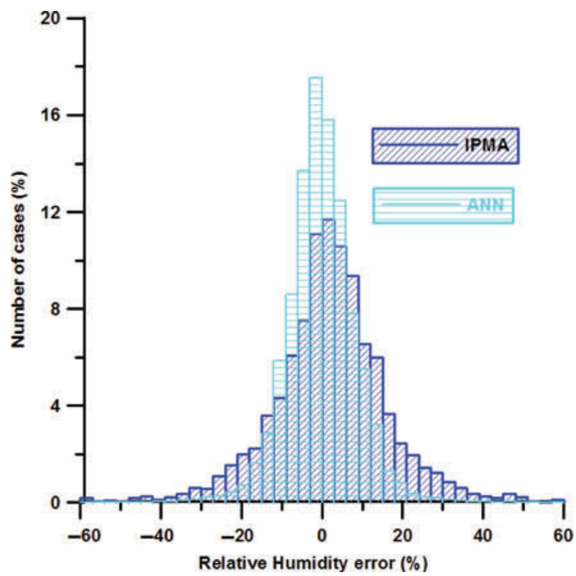

Figure 6. Distribution of errors of relative humidity retrieval at the 7.5 km altitude over water by means of two interpretation techniques, IPMA and ANN.

interpretation techniques, IPMA and MLR. These two distributions are very close, with RMS errors, respectively, of 15.8% and 18.8%. Figure 6 illustrates the evident advantage of the ANN technique as compared to the MLR (RMS errors for these two techniques are, respectively, 8.35% and 15.8%).

5. Conclusions

Interpretation of measurements of the outgoing thermal radiation by modern Fourier-spectrometers of high spectral resolution for temperature-humidity sensing of the atmosphere poses high requirements on the speed of performance in the procedures of in-line satellite measurement processing. One way to solve the performance speed problem is by using regression approaches, in particular, ANN. To reduce the problem dimension, the method of principal components can be used, in relation both to representation of the measured spectra and to the profiles of the meteorological parameters being retrieved. This allows substantial simplification of the application of the ANN technique in the process of creating it, reducing the number of coefficients determined.

In Russia, the advanced IR sounder IRFS-2 (InfraRed Fourier Spectrometer-2), designed and manufactured by Keldysh Centre (Roskosmos), is planned to be launched aboard the Meteor-M N 2 satellite in 2014.

In the present article, the algorithm of atmospheric temperature-humidity retrievals based on using ANNs is described, and this algorithm is compared with the traditional method of multiple linear regression and the iterative physical-mathematical approach for the Russian satellite Fourier Spectrometer IRFS-2.

As the characteristics of the retrieval accuracy, mean and RMS errors were used. The calculations allowed the following main conclusions to be drawn.

(1) The systematic errors of temperature retrieval for the ANN technique are practically equal to zero, and for the other techniques, they are not higher than 0.4 K. The MLR technique gives significant RMS errors in retrieval of the temperature profile, especially in the troposphere region; these errors may reach 2–3 K. The ANN and IPMA techniques are substantially more accurate, giving approximately equal RMS errors of 1.0–1.5 K at altitudes of 2–30 km. In all interpretation techniques, growth of the errors of temperature retrieval in the lower troposphere is observed, and this is especially substantial (up to 3 K for near-surface temperature) in temperature sensing over land. Taking into account that the *a priori* variability of temperature is 8–18 K at different altitudes for the database of temperature realisations used, the information content of the IRFS device with regard to the vertical temperature profile is, nevertheless, very high.

(2) The differences in temperature sensing of the atmosphere over water and land manifest themselves in the appearance of an additional five determined coefficients of expansion of the spectral dependence of IR emissivity of land in PC. This leads to the increase of the errors of temperature sensing in the lower troposphere, reaching ~0.5 K for all interpretation techniques.

(3) The variability of the errors of atmospheric temperature retrieval by means of the IRFS-2 device is substantially different at different altitudes in the atmosphere. Thus, for the near-surface temperature in the case of the water surface, the range of retrieval errors is rather wide for all interpretation techniques; for example, for the ANN technique, it is −6 to 8 K. For the near-surface temperature, the RMS errors for all techniques are approximately equal, at 2.3–2.5 K. In the free atmosphere at altitudes of 5, 10 and 20 km, the variability of the errors of temperature retrieval is substantially less, and the retrieval of temperature is carried out with substantially smaller RMS errors as compared to the near-surface layer. Thus, at the 5 km altitude, the range of error variability is −4 K to +4 K for the ANN technique, the mean square errors of the ANN and IPMA techniques being 0.85–

0.88 K. The MLR technique gives substantially larger error dispersion (−8 to +7 K).

(4) The information content of the IRFS-2 measurements with regard to the atmospheric humidity profile is relatively small, which is caused by high relative errors of measurements of the outgoing radiation in the shortwave range of the device measurements, particularly in the water vapour absorption band of 6.3 µm. In the case of observations over water, the mean errors for the ANN technique are practically equal to zero, and for the MLR and IPMA techniques, they are of approximately the same order of magnitude, at 2–4% of relative humidity. The ANN technique allows us to determine the relative humidity in the troposphere with relative errors of 10–15%. Approximately the same errors of retrieval of relative humidity are realized for the IPMA technique up to altitudes of ~6km. At higher altitudes, a substantial growth of errors of retrieval of relative humidity is observed for the IPMA and MLR techniques. In the upper troposphere, for the MLR technique, these errors approach 40%.

(5) Variations of the errors of relative humidity retrieval are significant for different interpretation techniques and for different altitudes in the atmosphere. The smallest variations, as well as the errors of retrieval of relative humidity themselves, were realized for the ANN technique at altitudes of ~5–8 km. Thus, for the altitude of 7.5 km in 90% of the cases, the errors of retrieval of humidity by means of the ANN techniques lie within the range ±15%, and the RMS error at this level for this technique is 8.4%, which is significantly smaller than for the MLR and IPMA techniques.

The main conclusion from these investigations of the efficiency of the interpretation technique based on using the ANNs is that this technique can successively replace not only the MLR at the first stage of analysis of satellite measurements, but also, in many cases, owing to its high accuracy, the IPMA technique.

Funding

The creating of the inverse codes was partly supported by Russian Foundation for Basic Research [grant number 12-05-00445]; Saint Petersburg State University [grant number 11.37.28.2011]. The numerical modelling and analysis were fulfilled with financial support of the Russian Science Foundation [grant number 14-17-0096].

References

Aires, F., A. Chedin, N. A. Scott, and W. B. Rossow. 2002. “A Regularized Neural Net Approach for Retrieval of Atmospheric and Surface Temperatures with the IASI Instrument.” *Journal of Applied Meteorology* 41: 144–159. doi:10.1175/1520-0450(2002)041<0144:ARNNAF>2.0.CO;2.

Aires, F., C. Prigent, W. B. Rossow, and M. Rothstein. 2001. “A New Neural Network Approach Including First Guess for Retrieval of Atmospheric Water Vapor, Cloud Liquid Water Path, Surface Temperature, and Emissivities over Land from Satellite Microwave Observations.” *Journal of Geophysical Research* 106: 14887–14907. doi:10.1029/2001JD900085.

Aires, F., W. B. Rossow, N. A. Scott, and A. Chedin. 2002a. “Remote Sensing from the Infrared Atmospheric Sounding Interferometer Instrument. 1. Compression, Denoising, and First-Guess Retrieval Algorithms.” *Journal of Geophysical Research* 107 (D22): 4619. doi:10.1029/2001JD000955.

Aires, F., W. B. Rossow, N. A. Scott, and A. Chedin. 2002b. “Remote Sensing from the Infrared Atmospheric Sounding Interferometer Instrument 2. Simultaneous Retrieval of Temperature, Water Vapor, and Ozone Atmospheric Profiles." *Journal of Geophysical Research* 107 (D22): 4620. doi:10.1029/2001JD001591.

Anderson, G. P., S. A. Clough, F. X. Kneizys, J. H. Chetwynd, and E. P. Shettle. 1986. *AFGL Atmospheric Constituent Profiles (0–120 Km)*. AFGL-TR-86-0110, Environmental Research Papers, No. 954, 43 p. Bedford, MA: AFGL (OPI), Hanscom AFB.

Aumann, H. H., M. T. Chahine, C. Gautier, M. D. Goldberg, E. Kalnay, L. M. McMillin, H. Revercomb, P. W. Rosenkranz, W. L. Smith, D. H. Staelin, L. Strow, and J. Susskind. 2003. "AIRS/AMSU/HSB on the Aqua Mission: Design, Science Objectives, Data Products, and Processing Systems." *IEEE Transactions on Geoscience and. Remote Sensing* 41: 253–264. doi:10.1109/TGRS.2002.808356.

Blackwell, W., J. Frederick, and W. Chen. 2005. "Neural Network Applications in High-Resolution Atmospheric Remote Sensing." *Lincoln Laboratory Journal* 15: 299–322.

Blackwell, W. J., M. Pieper, and L. G. Jairam. 2008. "Neural Network Estimation of Atmospheric Profiles Using AIRS/IASI/AMSU Data in the Presence of Clouds." In *Multispectral, Hyperspectral, and Ultraspectral Remote Sensing Technology, Techniques, and Applications II, Proceedings of SPIE*, vol. 7149, edited by A. M. Larar, M. J. Lynch, and M. Suzuki, 1–12. Noumea. doi:10.1117/12.821929.

Chedin, A., N. A. Scott, C. Wahiche, and P. Moulinier. 1985. "The Improved Initialization Inversion Method: A High Resolution Physical Method for Temperature Retrievals from Satellites of the TIROS-N Series." *Journal of Climate and Applied Meteorology* 24: 128–143. doi:10.1175/1520-0450(1985)024<0128:TIIIMA>2.0.CO;2.

Clerbaux, C., A. Boynard., L. Clarisse, M. George, J. Hadji-Lazaro, H. Herbin, D. Hurtmans, M. Pommier, A. Razavi, S. Turquety, C. Wespes, and P. Coheur. 2009. "Monitoring of Atmospheric Composition Using the Thermal Infrared Iasi/Metop Sounder." *Atmospheric Chemistry and Physics* 9: 6041–6054. doi:10.5194/acp-9-6041-2009.

Coheur, P.-F., L. Clarisse, S. Turquety, D. Hurtmans, and C. Clerbaux. 2009. "IASI Measurements of Reactive Trace Species in Biomass Burning Plumes." *Atmospheric Chemistry and Physics* 9: 5655–5667. www.atmos-chem-phys.net/9/5655/2009.

Frate, F. D., and G. Schiavon. 1998. "A Combined Natural Orthogonal Functions/Neural Network Technique for the Radiometric Estimation of Atmospheric Profiles." *Radio Science* 33: 405–410. doi:10.1029/97RS02219.

Gribanov, K. G., and V. I. Zakharov. 2003. "Neural Network Solution for Temperature Profile Retrieval from Infrared Spectra with High Spectral Resolution." *Atmospheric Science Letters* 5: 1–11. doi:10.1016/j.atmoscilet.2003.10.002.

Huang, H.-L., and P. Antonelli. 2001. "Application of Principal Component Analysis to High-Resolution Infrared Measurement Compression and Retrieval." *Journal of Applied Meteorology* 40: 365–388. doi:10.1175/1520-0450(2001)040<0365:AOPCAT>2.0.CO;2.

Kaplan, L. D. 1959. "Inference of Atmospheric Structure from Remote Radiation Measurements." *Journal of the Optical Society of America* 49: 1004–1006. doi:10.1364/JOSA.49.001004.

Karbou, F., F. Aires, C. Prigent, and L. Eymard. 2005. "Potential of Advanced Microwave Sounding Unit-A (AMSU-A) and AMSU-B Measurements for Atmospheric Temperature and Humidity Profiling over Land." *Journal of Geophysical Research* 110: D07109. doi:10.1029/2004JD005318.

King, Y. J. F. 1956. "The Earth Satellite Vehicle as a Stratospheric Temperature Probe." Proceedings of VII International Astronautical Congress, Rome, September 17–22.

Kondratyev, K. Y., and Y. M. Timofeev. 1970. *Thermal Sensing of the Atmosphere from Satellites*. Leningrad: Gidrometeoizdat. (NASA Technical Translation F-626.)

Krasnopolsky, V. M., G. H. Gemmill, and L. C. Breaker. 2000. "A Neural Network Multiparameter Algorithm for SSM/I Ocean Retrievals: Comparisons and Validations." *Remote Sensing of Environment* 73: 133–142.

Liu, X., D. K. Zhou, A. M. Larar, W. L. Smith, P. Schluessel, S. M. Newman, J. P. Taylor, and W. Wu. 2009. "Retrieval of Atmospheric Profiles and Cloud Properties from IASI Spectra Using Super-Channels." *Atmospheric Chemistry and Physics* 9: 9121–9142. doi:10.5194/acp-9-9121-2009.

Matricardi, M. 2004. *RTIASI-5 User's Guide*, 47 pp. Report EUMETSAT. Contract EUM/CO/02/989/PS, Reading: ECMWF.

Matricardi, M., and R. Saunders. 1999. "Fast Radiative Transfer Model for Simulation of Infrared Atmospheric Sounding Interferometer Radiances." *Applied Optics* 38: 5679–5691.

Nalli, N. R., W. L. Smith, and B. Huang. 2001. "Quasi-Specular Model for Calculating the Reflection of Atmospheric Emitted Infrared Radiation from a Rough Water Surface." *Applied Optics* 40: 1343–1353. doi:10.1364/AO.40.001343.

Polyakov, A. V. 1996. "On Using a Priori Statistical Information in Solving Non-Linear Inverse Problems of Atmospheric Optics." [In Russian.] *Issledovaniya Zemli Iz Kosmosa* 3: 11–17.

Polyakov, A. V. 2014. "The Method of Artificial Neural Networks in Retrieving Vertical Profiles of Atmospheric Parameters." *Atmospheric and Oceanic Optics* 27: 247–252.

Polyakov, A. V., Y. M. Timofeyev, and A. B. Uspenskiy. 2009. "Temperature-Humidity Sounding of the Atmosphere by the Data of a Satellite Sensor of High Spectral Resolution IRFS-2." [In Russian.] *Issledovaniya Zemli Iz Kosmosa* 5: 3–10.

Polyakov, A. V., Y. M. Timofeyev, and A. B. Uspenskiy. 2010. "Possibilities of Determination of Temperature and Emissivity of the Land Surface by the Data of Satellite Sensors of High Spectral Resolution (IRFS-2)." [In Russian.] *Issledovaniya Zemli Iz Kosmosa* 4: 85–90.

Pougatchev, N. T., X. August, T. Calbet, O. Hultberg, P. Oduleye, B. Schlüssel, G. Stiller, K. St. Germain, and G. Bingham. 2009. "IASI Temperature and Water Vapor Retrievals – Error Assessment and Validation." *Atmospheric Chemistry Physics* 9: 6453–6458.

Smith Sr., W. L., H. Revercomb, G. Bingham, A. Larar, H. Huang, D. Zhou, J. Li, X. Liu, and S. Kireev. 2009. "Technical Note: Evolution, Current Capabilities, and Future Advance in Satellite Nadir Viewing Ultra-Spectral IR Sounding of the Lower Atmosphere." *Atmospheric Chemistry Physics* 9: 5563–5574. doi:10.5194/acp-9-5563-2009.

Smith, W. L., E. Weisz, S. Kirev, D. K. Zhou, Z. Li, and E. E. Borbas. 2012. "Dual-Regression Retrieval Algorithm for Real-Time Processing of Satellite Ultraspectral Radiances." *Journal of Applied Meteorology and Climatology* 51: 1455–1476.

Timofeyev, Y. M., and A. A. Martynov. 1996. "On Determination of Temperature and Emissivity of Land Surface." [In Russian.] *Issledovaniya Zemli Iz Kosmosa* 4: 12–17.

Uspenskiy, A. B., S. V. Romanov, and A. N. Trotsenko. 2003. "Application of the Method of Main Components for Analysis of Satellite-Measured IR Spectra of High Resolution." [In Russian.] *Issledovaniya Zemli Iz Kosmosa* 3: 26–33.

Virolainen, Y. A., Y. M. Timofeyev, A. V. Polyakov, and A. B. Uspenskiy. 2010. "Optimal Parametrization of Spectra of Outgoing Thermal Radiation by the Example of Data of the Satellite IR-Sensor IRFS-2." [In Russian.] *Optika Atmosfery I Okeana* 23: 143–148.

Wang, N., Z.-L. Lia, B.-H. Tanga, F. Zengd, and C. Lie. 2013. "Retrieval of Atmospheric and Land Surface Parameters from Satellite-Based Thermal Infrared Hyperspectral Data Using a Neural Network Technique." *International Journal of Remote Sensing* 34: 3485–3502. http://dx.doi.org/10.1080/01431161.2012.716536.

Zavelevich, F. S., Y. M. Golovin, and A. V. Desyatov. 2009. "The Engineering Unit of the On-Board Infrared Fourier Spectrometer IRFS-2 for Temperature and Humidity Sensing of the Atmosphere of the Earth." [In Russian.] *Proceedings of All-Russia conference "Present-day problems of remote sensing of the atmosphere from space"* 1 (6): 259–266. M., IKI RAN, 10–14 November 2008. Collection of scientific articles. M., "Azbuka-2000".